Z. Physik B 36, 161–177 (1979)

Zeitschrift
für Physik B

Phase Diagrams and Magnetic Properties of Diluted Ising and Heisenberg Magnets with Competing Interactions

K. Binder and W. Kinzel
Institut für Festkörperforschung, Kernforschungsanlage Jülich, Jülich, Fed. Rep. Germany

D. Stauffer
Institut für Theoretische Physik, Universität Köln, Köln, Fed. Rep. Germany

Received August 1, 1979

Ising and Heisenberg magnets with nearest-neighbor ferromagnetic exchange J_1 and next-nearest antiferromagnetic exchange J_2 and randomly distributed frozen-in nonmagnetic impurities of arbitrary concentration $1-x$ are studied by several methods: systematic series expansions in x, $1-x$ and inverse temperature $(1/T)$ as well as Monte Carlo simulation. Depending on $R \equiv J_2/J_1$, T and x the model is in paramagnetic, ferromagnetic, antiferromagnetic or spin glass phases. The microscopic magnetic structures of all these phases are investigated and found to be more complicated than usually (e.g., the ferromagnetic state contains spins and clusters either aligned antiparallel or not aligned at all, when "frustration" effects make bonds ineffective). We suggest that the concentration x_c of magnetic ions below which no (anti-)ferromagnetic long range order occurs depends on R continuously, and $x_c \to 1$ at the multicritical point (R_m, $T=0$) where the order changes from ferromagnetic to antiferromagnetic. Our results for phase diagram, susceptibility etc. are compared to recent data on the $Eu_xSr_{1-x}S$ system and very good agreement is found.

I. Introduction

Recently there has been very much interest in the properties of systems with quenched disorder [1–4], e.g. magnets diluted at random with nonmagnetic impurities. If the magnetic interactions are purely ferromagnetic and the dilution amounts to just remove spins (i.e., no significant change of lattice parameter, electronic structure etc. occurs and hence the exchange constants between the remaining spins remain unaltered), one finds that magnetic long-range order occurs for concentrations x of the magnetic ions exceeding the percolation threshold x_p, while for $x < x_p$ only finite (superparamagnetic) clusters occur. It is well known that x_p depends on the geometry of the lattice and range of interaction only, but is independent of interaction strengths, anisotropy (i.e., the same for the Ising and the Heisenberg case), spin quantum number, etc. Both the properties of the percolation transition as x approaches x_p [5] and the magnetic transition as T approaches $T_c(x)$ [6] are fairly well understood.

The situation is much more complicated if competing magnetic interactions occur, even if a ferromagnetic phase is stable in the nondiluted system due to sufficiently strong ferromagnetic nearest neighbor exchange J_1. One then finds that a spin glass phase occurs for a regime of concentrations up to x_c, where x_c sometimes exceeds the nearest-neighbor percolation threshold x_p^{nn} only slightly (e.g. in Fe diluted with Au [7]) and sometimes x_c exceeds x_p^{nn} distinctly (e.g. in $Eu_xSr_{1-x}S$ [8]). For a certain range of x the system upon cooling first orders ferromagnetically and at lower temperatures exhibits a second transition to a spin glass phase which there is the magnetic ground state [7, 8]. It must be noted, however, that at present there is no agreement whether the spin glass state is a "phase" in the sense of true

0340-224X/79/0036/0161/$03.40

thermodynamic equilibrium or whether spin glass freezing is only a nonequilibrium effect [2, 9]. In fact, superparamagnetic clusters are frequently invoked to explain this phenomenon [10], while the common theoretical models employ Ising or Heisenberg models with bond disorder rather than site disorder [2, 9]. Clearly, picturing a spin glass as an assembly of noninteracting clusters of suitable sizes whose magnetic moments experience suitable anisotropy barriers [10] one has enough parameters at ones disposal to reasonably fit experimental data; but we feel that this procedure does not really provide the desired theoretical explanation of the phenomena considered. On the other hand, the Edwards-Anderson model [2, 9, 11] with gaussian distribution of exchange between nearest neighbors on a lattice hardly explains any experimental data *quantitatively*, although computer simulations showed that it agrees with experiment *qualitatively* [2, 4]. In order to reconcile it with experiment, it was suggested [12] to reinterpret it as a model of randomly interacting clusters rather than randomly interacting individual spins. Making this reinterpretation quantitative one would have to determine the distribution of cluster size, magnetic moment etc. from a microscopic theory. We feel that this task is too complicated for materials like Au–Fe or Cu–Mn in the vicinity of the respective percolation concentrations: there deviations from random mixing are expected in these materials [10]; and hence the precise distribution of "chemical clusters" is unknown; mean-free path effects could already affect the long-range indirect Ruderman Kittel exchange at these concentrations, while electronic correlation effects could affect both the atomic moments and the direct exchange of the magnetic atoms. Therefore we concentrate here on insulating systems like $Eu_xSr_{1-x}S$, where such electronic effects do not occur, and there are good reasons to believe that atomic moments and exchange constants do not depend on x [13]. In addition, this system experimentally can be produced for arbitrary x and ample evidence for the random character of mixing exists [13, 14]. Hence the distribution of clusters is just that of the site percolation problem.

This is our motivation to study diluted Ising- and Heisenberg magnets with nearest neighbor ferromagnetic and next nearest neighbor antiferromagnetic exchange, which is the simplest site-disorder problem exhibiting nontrivial spin glass behavior and at the same time provides a quantitatively accurate representation of real materials. In the extremely dilute regime ($x \ll x_p^{nnn}$) this approach has already been used to quantitatively identify contributions due to superparamagnetic clusters in the frequency-dependent susceptibility [14]. The blocking of the clusters was shown to be due to intracluster dipolar anisotropy, while the intercluster dipolar coupling gives rise to a dipolar-spin glass freezing at very low temperatures. In the present paper where much higher concentrations are considered and the temperatures of interest are orders of magnitude higher, dipolar interactions are less important and will be disregarded.

Our paper is organized as follows. In Sect. II the ground state properties of our systems are considered, concentrating on the case of an Ising square lattice. In Sect. III results for nonzero temperature based on both high temperature expansions and Monte Carlo simulations are described. Section IV contains a detailed discussion of experimental data for $Eu_xSr_{1-x}S$ [8, 13, 15, 16] in the light of our theory, while Sect. V contains our conclusions. Some aspects of this approach have very briefly already been described in Ref. 2, 16, 17. Our computational details on concentration expansions are found in Appendix A and on high temperature expansions in Appendix B.

II. Ground State Properties

Let us first consider an Ising square lattice with $J_1>0$, $J_2<0$ at $T=0$. The nondiluted system is ferromagnetic for $R \equiv J_2/J_1 > R_m = -1/2$, while it has a layered antiferromagnetic ("superantiferromagnetic") structure for $R<R_m$. For $x<x_p^{nnn}$ the state consists of an arrangement of finite clusters, a few of which are shown in Fig. 1. Some clusters have a ferromagnetic ground state (Fig. 1 A), while for other clusters some spins are aligned antiparallel (Fig. 1 B). There are also configurations of spins ($C1$, $C2$) where the ground state depends on R: the cluster shown has all spins parallel for $R>-\frac{1}{2}$, while one spin aligns antiparallel to the other ones for $R<-\frac{1}{2}$. At the multicritical value $R_m=-\frac{1}{2}$ the ground state of this cluster is degenerate, because both possibilities $C1$, $C2$ have then the same energy. With respect to the contribution of this cluster to magnetic properties this cluster for $R=R_m$ effectively behaves as if it were "split" into two independent smaller clusters (in this case one cluster containing 4 spins and a single spin).

Even more interesting is the behavior of the cluster shown in Fig. 1 D. For $R>-\frac{1}{2}$ the ferromagnetic bonds will align the three spins in the left lower part of this cluster parallel to each other, irrespective of the configuration of the remaining spins, which are coupled to this cluster only by antiferromagnetic bonds. Since it is impossible to satisfy the three antiferromagnetic bonds at the same time, there are

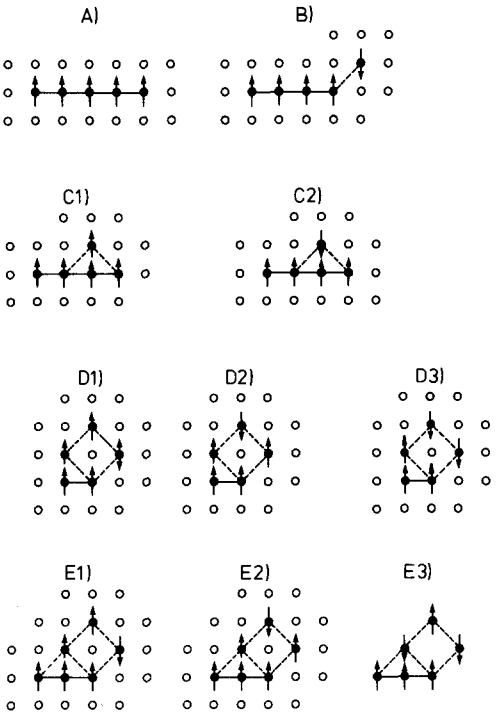

Fig. 1. Ground state configurations of various clusters of magnetic atoms (black dots). Nonmagnetic atoms are shown as open circles, nearest-neighbor bonds are indicated by full and next-nearest neighbor bonds by broken lines. For further explanations cf. text

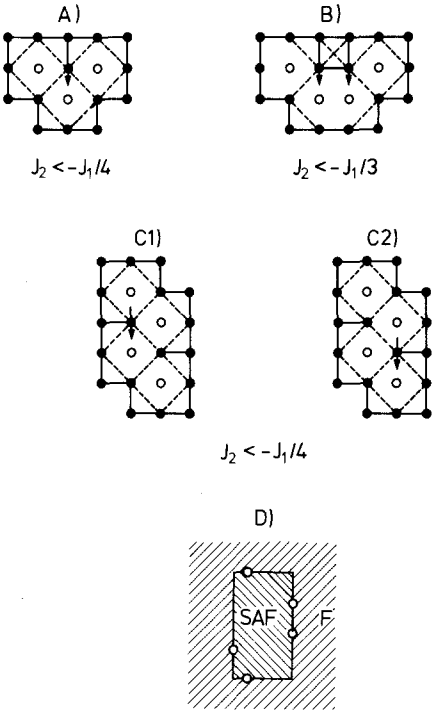

Fig. 2. Reversed spins in the vicinity of nonmagnetic impurities (open circles) occurring in the ferromagnetic region of a diluted system of magnetic atoms (black dots). Nearest-neighbor bonds are indicated by full and next-nearest neighbor bonds by broken lines. For further explanations cf. text

three degenerate spin configurations $D1$, $D2$, $D3$. Hence for arbitrary R in the range $-\frac{1}{2}<R<0$ this cluster has a 6-fold ground state degeneracy, rather than the usual 2-fold Ising degeneracy of the clusters shown in Fig. 1A–C. For $R<-\frac{1}{2}$ the antiferromagnetic bonds overrule the ferromagnetic ones, i.e. the 4 spins of the next-nearest neighbor square will order antiferromagnetically. The 5th spin (in the left lower corner of this cluster) is then effectively decoupled from the rest because this spin can point up or down with equal probability for all $R<-\frac{1}{2}$. Hence for $R<-\frac{1}{2}$ the cluster of Fig. 1D has a 4-fold degeneracy. For $R=R_m=-\frac{1}{2}$ again all these ground states for $R<-\frac{1}{2}$ and $R>-\frac{1}{2}$ become equivalent, which yields an even larger ground state degeneracy, and a smaller degree of spin correlation in that cluster. Also for other R due to the degeneracy the average correlation for some pairs of spins has a reduced value. We will return to the appropriate definition of susceptibilities measuring these correlations below.

While for clusters containing only up to five spins there is only one special value of R (namely R_m) where an enhanced degeneracy occurs, larger clusters exhibit enhanced degeneracy also for other rational values of R. E.g., the cluster of six spins shown in Fig. 1E has a degenerate ground state ($E1$, $E2$, and another configuration not shown) for $R>-\frac{1}{3}$, while for $R<-\frac{1}{3}$ there is only one nondegenerate ground state configuration ($E3$), and for $R=-\frac{1}{3}$ all these states are degenerate.

Before we try to draw more quantitative conclusions let us consider the opposite limit, $x\to 1$, where the system is expected to have a ferromagnetic ground state. There we have to consider the effect of localized impurities or small clusters of impurities on the local magnetic order in their environment only, Fig. 2. There it may occur that ferromagnetic bonds are overruled by antiferromagnetic ones: e.g., for $R<-\frac{1}{4}$ the spin close to the impurity configuration of Fig. 2A orders antiparallel to the remaining ferromagnetic net, while for $R>-\frac{1}{4}$ it stays parallel, and for $R=-\frac{1}{4}$ both orientations of this spin are degenerate. Similarly in Fig. 2B we have an antiparallel "dimer" (i.e., cluster containing two spins) for $R<-\frac{1}{3}$, which becomes effectively decoupled from the ferromagnetic net for $R=-\frac{1}{3}$ and ferromagnetically aligned for $R>-\frac{1}{3}$. Similarly configurations containing a larger number of close-by impurities may give rise to larger and larger antiparallel clusters. Most interesting, however, is the defect configuration of Fig. 2C: there it is favorable to have either one of two spins antiparallel to the ferromagnetic network provided $R<$

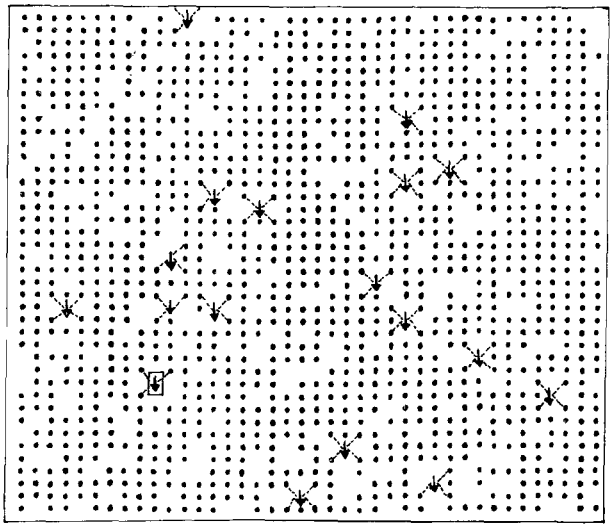

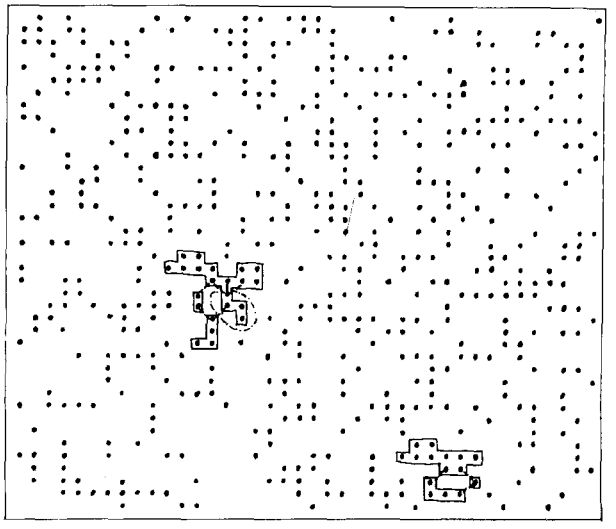

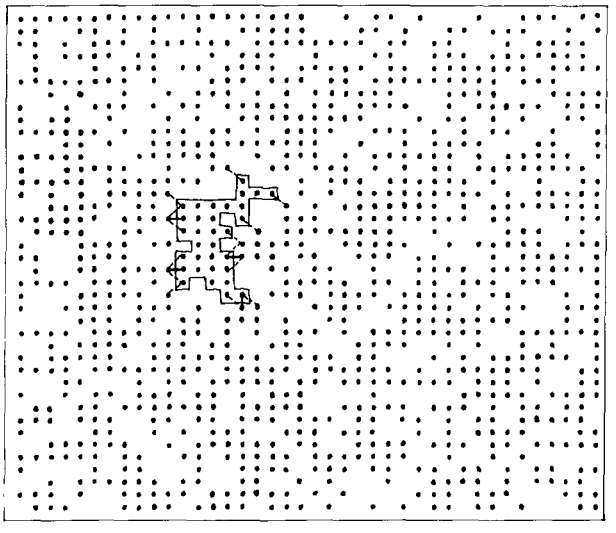

Fig. 3A–C. Monte Carlo generated 40×40 lattices at concentrations $x=0.82$ (**A**), $x=0.66$ (**B**) and $x=0.35$ (**C**). Magnetic atoms are shown as black dots, nonmagnetic atoms are not shown. Nearest-neighbor bonds are indicated by full and next-nearest neighbor bonds by broken lines. For further explanation cf. text

$-\frac{1}{4}$, but it is undecided which of them and hence the states $C1$, $C2$ are degenerate. As a result, the ferromagnetic state of such a diluted Ising system with competing interactions has an enhanced ground-state entropy. We may view the effect of the impurity configuration in Fig. 2C to split off an antiferromagnetic dimer from the ferromagnetic net. As a result of the effects considered in Fig. 2, less spins contribute to the magnetization of the percolating network than would be expected on purely geometric grounds.

A particularly interesting case occurs in the immediate vicinity of the multicritical point $R_m=\frac{1}{2}$ and very low impurity concentration ($x\to 1$). For $R=R_m$ not only the bulk energies of the ferromagnetic and superantiferromagnetic phases become equal, but also their interface energy (in the ground state) vanishes [18]. Nevertheless in the ground state of the pure system ($x=1$) at $R=R_m$ there cannot occur any clusters having all linear dimensions finite, since their corners still would cost energy. In the presence of nonmagnetic impurities, however, it is possible to create e.g. finite domains of superantiferromagnetic (SAF) phase in a ferromagnetic (F) environment: if the domain walls suitably cross by close to impurity sites (Fig. 2D) energy is won similarly as in Fig. 2A–C there, and this energy may compensate the unfavorable corner energy of the domains. Note that this argument holds for arbitrarily small dilution since then only the size of the domains must become large enough. As a result, we expect the lines separating the ferromagnetic (or superantiferromagnetic) phase from the spin glass phase to come together in the multicritical point $R=R_m$, $x=1.0$ (see Fig. 4 below).

We now consider the effect that the impurities have on the magnetic order when one no longer considers isolated impurity configurations but rather a finite impurity concentration in a large lattice. Figure 3 shows several Monte Carlo samples of a 40×40 lattice where sites were filled at random by magnetic atoms (black dots) at concentration x. At $x=0.82$ (Fig. 3A) there is one spin (encircled), which is reversed for all $-\frac{1}{2}<R<0$, while the other reversed spins shown are reversed for $R<-\frac{1}{4}$ (corresponding to Fig. 2A) or for $R<-\frac{1}{3}$ (if a next-nearest site of the reversed spin is missing). At $x=0.66$ (Fig. 3B) we are definitely beyond the nearest-neighbor percolation threshold ($x_p^{nn}=0.59$ on the square lattice [19]), and hence most of the spins do belong to the percolating network. But it is easy to see that for suitably negative R the ground state of this network is not fer-

romagnetic: e.g., overturning the encircled group of atoms we break four ferromagnetic bonds but at the same time 14 antiferromagnetic bonds become satisfied. Thus it would be unfavorable if this group of atoms would align parallel to its environment. Thus, for $R<-\frac{4}{14}$ this cluster of spins will be aligned antiparallel to its environment. It is easy to identify many other clusters of spins which align antiparallel to their environment for $R<-l/m$, where the numbers l, m of unfavorable ferromagnetic and favorable antiferromagnetic bonds can be found by simple counting. As a result, one can convince oneself that the percolating network in Fig. 3B is completely split into many ferromagnetic clusters of intermediate size which want to align antiparallel to each other. Of course, due to their mutual interactions it is not possible in general to find an arrangement which is satisfactory to all these clusters: a lot of bonds between the clusters will be "frustrated" [20] and hence a uniquely aligned state of this spin glass phase does not exist. There will be several ways by which the percolating net is cut into "clusters" aligned antiparallel to each other which yield the same ground-state energy. In addition to this "*global degeneracy*" of the spin glass phase there will be similar *local* degeneracy effects as have been found for small clusters (Fig. 1D) and in the ferromagnetic phase (Fig. 2C).

Figure 3C shows a configuration at $x=0.35$, i.e. close to the next-nearest neighbor percolation threshold ($x_p^{nnn}=0.41$ on the square lattice [19]). Ferromagnetic clusters are coupled together by antiferromagnetic bonds to form larger clusters of the spin glass phase. But again it occurs that the resulting larger clusters are degenerate (like the one marked in the upper part, where three ferromagnetic clusters are coupled together by three antiferromagnetic bonds in a configuration corresponding to an antiferromagnetic triangle). It also happens that antiferromagnetic bonds in these coupled clusters turn over parts of the original ferromagnetic clusters (like the one encircled with a dash-dotted line). As a result, geometric nearest and next-nearest neighbor percolation are not expected to have much influence on magnetic properties here: the essential point is to minimize the energy by suitable *magnetic* clusters which do not coincide with the *geometric* ones, but are derived from counting favorable and unfavorable bonds. I.e., a "*geometric cluster*" is a group of spins connected by exchange forces, while a "*magnetic clusters*" is a group of spins with fixed relative orientations at $T=0$.

These considerations lead us to draw the *qualitative* ground-state phase diagram in Fig. 4. At $R\to 0$ the boundary x_c' between paramagnetic and spin glass phases (dash-dotted curve) starts out at x_p^{nnn}, but for $R<0$ we expect that $x_c'>x_p^{nnn}$, and we speculate that

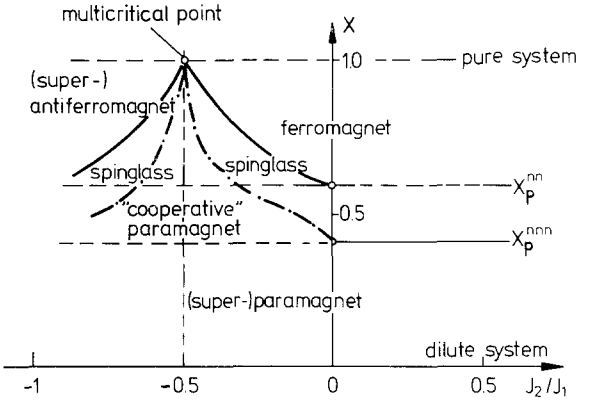

Fig. 4. Schematic ground state phase diagram of the diluted Ising square. Full curve denotes x_c'' while dashdotted curve denotes x_c'

$x_c'\to 1$ for $R\to R_m$. For $x_p^{nnn}<x<x_c'$ there is geometric percolation but there is no long-range spin correlation in the ground state, the system is a kind of "cooperative paramagnet" [21]. As $x\to x_c'$ larger and larger magnetic clusters are formed. Since the bond counting for very large clusters yields different answers for the magnetic structure of the cluster depending whether $R>R_{lm}=-l/m$ or $R<R_{lm}$, and l, $m\to\infty$ as the cluster size diverges, the set of critical values $\{R_{lm}\}$ is quasicontinuous. Hence we expect x_c' to be a more or less smooth function of R, although we can not exclude that there are certain singularities in higher derivatives of x_c' with respect to R at these values $\{R_{lm}\}$ (which should be most pronounced if both l and m are small). A similar behavior we expect for the boundary x_c'' between spin glass and ferromagnetic phase, apart from the fact that it starts out at x_p^{nn} for $R\to 0$. In the regime of the spin glass phase ($x_c'<x<x_c''$) the size of ferromagnetically ordered regions is finite although there is long-range magnetic correlation. From Fig. 3 we expect that the size of these ferromagnetic clusters within the spin-glass phase diverges when $x\to x_c''$, and the magnetization at $x\gtrsim x_c''$ sets in continuously rather than via a first-order transition.

In order to put these ideas on a more quantitative basis, we may investigate the behavior of ferromagnetic and spin glass susceptibilities in the disordered phase [2]

$$k_B T\chi_F=(\sum_{ij}\langle S_i S_j\rangle_T)/N, \tag{1a}$$

$$k_B T\chi_{EA}=(\sum_{ij}\langle S_i S_j\rangle_T^2)/N, \tag{1b}$$

and [22]

$$k_B T\chi_{SG}=(\sum_{ij}\langle S_i S_j\rangle_0\langle S_i S_j\rangle_T)/N. \tag{1c}$$

For $T=0$ there is no difference between χ_{EA} and χ_{SG}, of course. For $R<-\frac{1}{2}$ it is also interesting to study a susceptibility sensitive to superantiferromagnetic (SAF) ordering $\left\{\mathbf{Q}_1=\frac{\pi}{a}(1,0), \mathbf{Q}_2=\frac{\pi}{a}(0,1),\ a \text{ is the lattice spacing}\right\}$

$$k_B T \chi_{\mathrm{SAF}}=\Big(\sum_{ij} e^{i\mathbf{Q}_1(\mathbf{r}_i-\mathbf{r}_j)}\langle S_i S_j\rangle_T + \sum_{ij} e^{i\mathbf{Q}_2(\mathbf{r}_i-\mathbf{r}_j)}\langle S_i S_j\rangle_T\Big)/N. \tag{1d}$$

We hence want to calculate these susceptibilities as a function of R and x and by locating a divergence find the lines $x_c'(R)$ and $x_c''(R)$. In Appendix A this is attempted by a systematic expansion of both $k_B T\chi_F$ and $k_B T\chi_{EA}$ in powers of x, and coefficients up to order x^9 are obtained. However, since up to that order only clusters with at most 9 spins contribute, only changes at R_{lm} with *small* l, m can show up in these coefficients, and therefore an extrapolation of such series *in principle* is unable to clearly reveal the continuous variation of x_c' and x_c'' with R. It is also doubtful that a meaningful estimation of x_c'' is possible at all, since the onset of a spin glass order parameter at $x>x_c'$ should affect $k_B T\chi$ and hence the concentration where $k_B T\chi$ diverges is changed. There is even doubt that a meaningful extrapolation of the series beyond x_p^{nnn} is possible [23]: just as in a dilute magnet Griffiths singularities [24] occur for $T_c(x)<T<T_c(1)$, one expects related singularities for $x_p^{nnn}<x<x_c'$ in our problem. Of course, neither a ratio analysis nor a Padé approximant analysis appropriately handles such singularities. As a matter of fact, both the series for x_c' and x_c'' are very illbehaved, and extrapolation yielded rather crude estimates of $x_c'(R)$ and $x_c''(R)$ only (Fig. 5). Within our accuracy $x_c'(R)$

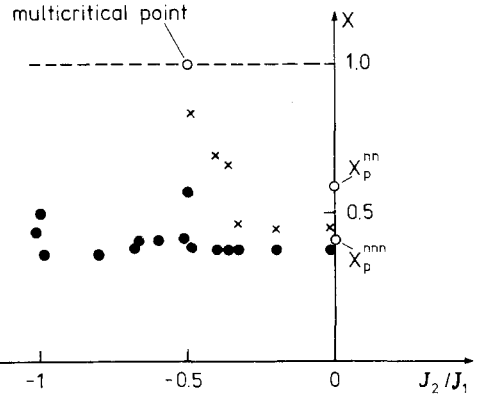

Fig. 5. Ground state phase diagram of the diluted Ising square as obtained from the series analysis. Dots are the Padé estimates for the transition paramagnet-spin glass (x_c'), crosses are the Padé estimates for the transition spin glass-ferromagnet (x_c'')

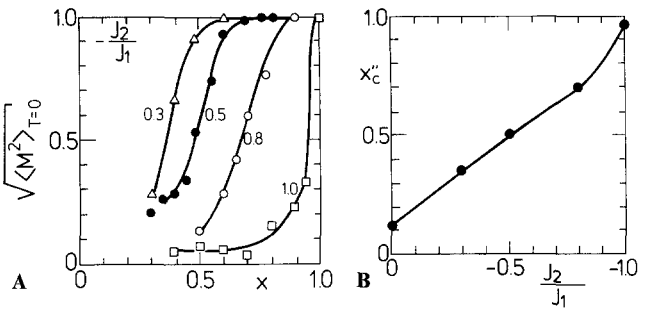

Fig. 6. A Ground state magnetization of a classical fcc Heisenberg ferromagnet as a function of concentration as obtained from Monte Carlo simulation. **B** Variation of the $T=0$ phase boundary between spin glass and ferromagnet (x_c'') as obtained from simulation

and x_p^{nnn} coincide except for $R=R_m$, where x_c' is enhanced but little evidence is provided that actually $x_c'(R_m)=1$. We further find that $x_c''>x_c'$, as expected, possibly approaching unity for $R\to R_m$.

An alternative to this series expansion from the disordered regime {where one systematically counts the contributions of all clusters as shown in Fig. 1 to the susceptibilities in Eq. (1)} is an expansion of the magnetization M in powers of $y=1-x$, by systematically considering all possible defect configurations in a ferromagnetically ordered phase (Fig. 2). The resulting series is also quoted in Appendix A. In principle, one could locate x_c'' by looking for a pole in the derivative $\partial M/\partial y$, but in practice our series are too short to yield meaningful estimates. Note also that this method again implicitly assumes the $T=0$ spin glass-ferromagnet transition to be of second order.

More satisfactory accuracy can be obtained utilizing Monte Carlo methods (for details on this method see [4]) Fig. 6A shows the magnetization of classical fcc Heisenberg ferromagnets as a function of x for various values of $-R$. In this case $R_m=-1$, and as expected the magnetization breaks down with very small impurity concentration here. Of course, the Monte Carlo simulation deals with a finite system (typically $N\approx 10^3$ spins), and hence there is a nonzero "finite size-tail" in the magnetization for $x<x_c''$: the root mean square magnetization shown here is just $\sqrt{k_B T\chi_F/N}$ in this region. The strong increase of this quantity as $x\to x_c''$ is consistent with a divergence of χ_F there, as conjectured above. The smooth decrease of M as x is lowered for $R>R_m$ is consistent with a second-order transition, too, although the finite size effects are too large to definitely rule out a first-order transition. Figure 6B shows then our final estimate for $x_c''(R)$, which indeed seems to be an extremely smooth function of R.

We expect a similar behavior also for the $d=3$ Ising case, apart from the fact that $T_c(R_m)\neq 0$ there and

presumably also $x_c'(R_m) < 1$. Even more complicated is the microscopic spin structure for the $d=3$ Heisenberg model. Apart from antiparallel spins one expects also canted spin configurations; moreover, due to the much larger number of nearest neighbors in the fcc lattice the effects shown in Fig. 2 can occur only in much higher order of $(1-x)$: e.g., 7 rather than 3 close by impurities are needed to allow for a spin aligned antiferromagnetically in the ferromagnetic phase, etc. In view of these difficulties we do not attempt to extend our concentration expansions to the ground state of Heisenberg magnets.

III. The Transition from the Paramagnetic to the Ferromagnetic Phase

While concentration expansions (Appendix A) seem to work well at both $T=0$ and nonzero temperature for noncompeting exchange [25, 26], our ground-state results have shown that this method is very problematic for competing exchange. Hence we did not attempt to extend it to nonzero temperature here, but restrict ourselves to the use of high temperature series expansions (for technical details see Appendix B) and Monte Carlo methods. While the high temperature expansion technique [27] has been fairly useful for diluted Ising systems [28], for diluted Heisenberg systems this method has been very problematic [29, 30]: due to erratic behavior of the series no reliable estimates of $T_c(x)$ could be obtained for $x \lesssim 0.5$, using nearest neighbor exchange only. In our case of competing interactions, where only terms including 4^{th} order in $(1/k_B T)$ are available (Appendix B), the series becomes already somewhat irregular for $x < 0.7$, Fig. 7. There a plot of the successive ratios a_l/a_{l-1} versus order of expansion l is given, where a_l are the expansion coefficients of the susceptibility. As is well known, for $l \to \infty$ these ratios should follow a straight line, whose intercept with the ordinate yields T_c, while from the slope one can get the susceptibility exponent γ [27]. Clearly, with such a limited number of terms a meaningful estimation of the asymptotic critical behavior is not possible, and hence we regard our exponent estimates γ_{eff} only as "effective susceptibility exponents" describing the apparent critical behavior not too close to T_c. A similar expansion for the correlation length was performed also, the ratio plot looks very similar to Fig. 7 again and yields results consistent with that of the susceptibility.

From Fig. 7 we observe that the series are well-behaved for $x \gtrsim 0.7$, and also the exponent γ_{eff} stays close to about 1.4 (which is not too different from the expected asymptotic value $\gamma = 1.38$ [31]), while

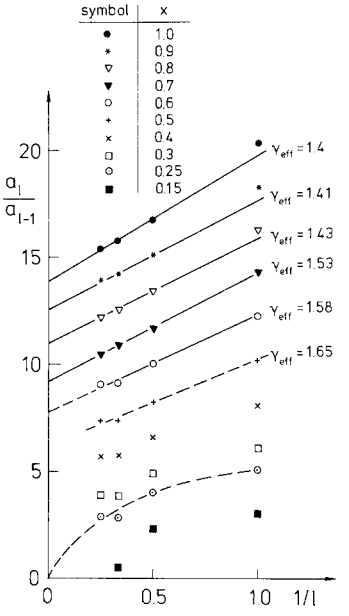

Fig. 7. Ratio plot for the susceptibility of an fcc $S=\frac{7}{2}$ Heisenberg ferromagnet, with $J_2=-J_1/2$, paramagnetic Curie temperature $\Theta=20.3$ K. Various concentrations x are shown

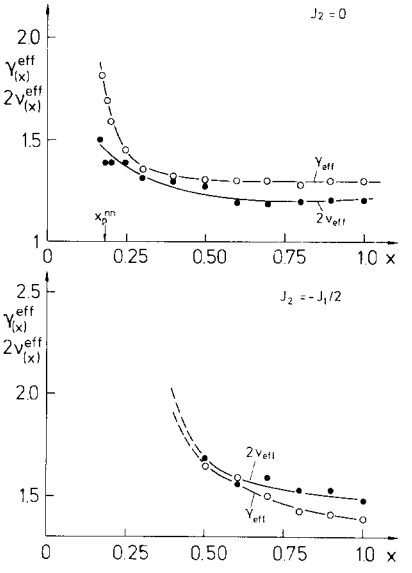

Fig. 8. Effective exponents of susceptibility (γ_{eff}) and correlation length (ν_{eff}) plotted versus concentration x for $R=0$ (upper part) and $R=-\frac{1}{2}$ (lower part)

around $x \approx 0.5$ the series start to become irregular and the exponents start to increase distinctly, Fig. 8. For $x=0.5$ to 0.3 the series are too erratic to yield any conclusive answer, while it is fairly clear from Fig. 7 that $T_c(x)=0$ for $x \leqq 0.25$.

It is interesting to compare this behavior inferred from a very short series to that of a nearest-neighbor Heisenberg ferromagnet, analyzed with the same

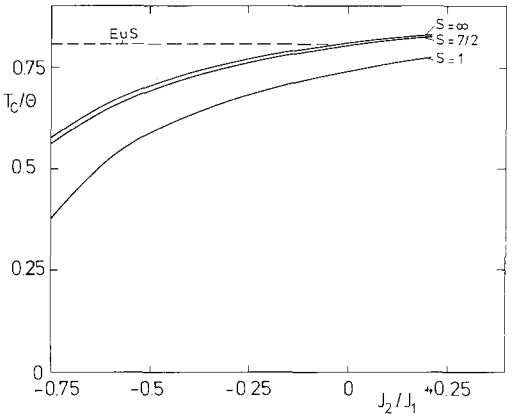

Fig. 9. T_c/Θ plotted versus R for several values of spin quantum number S. The literature value for EuS $T_c/\Theta=0.81$ [33] is indicated by the broken horizontal line

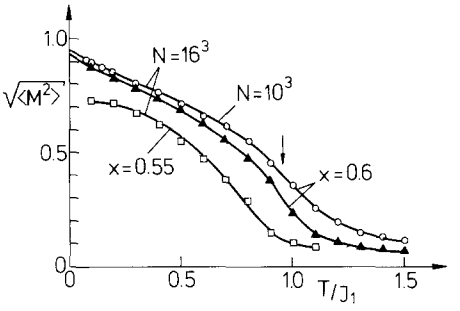

Fig. 10. Root mean square magnetization for an fcc classical Heisenberg ferromagnet with $R=-\frac{1}{2}$ plotted versus temperature. The arrow marks the estimate for T_c in the case of $x=0.6$

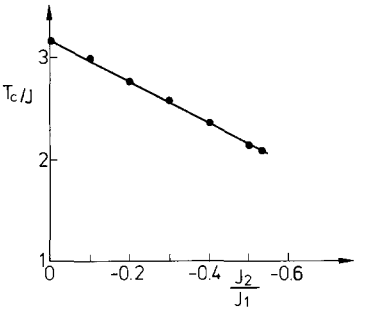

Fig. 11. Monte Carlo estimates for the critical temperature T_c of a classical fcc Heisenberg ferromagnet with both nearest (J_{nn}) and next nearest (J_{nnn}) interactions

number of terms. There one finds (Fig. 8) that the effective exponents stay more or less constant for $x \geqq 0.3$, while at $x=0.2$ they increase strongly {$T_c(0.2)$ extrapolated from just 4 terms would still be distinctly nonzero}. In this case, however, it is well known that $T_c(x) \to 0$ for $x \to x_p^{nn}=0.198$ [19]. Since the percolation threshold is a multicritical point [1], the behavior seen in Fig. 8 is just an indication of the crossover phenomena occurring there. By the same token, we may conclude that that for $R=-\frac{1}{2}$ ferromagnetism must break down for x close to 0.5, where the increase of exponents also indicates that a crossover region is reached.

This suggestion is confirmed by Monte Carlo calculations on a classical ($S \to \infty$) fcc Heisenberg spin system. First we note from series expansions for different S at $x=1$ where terms up to $(1/k_BT)^6$ are available [32], that T_c/Θ for $S=\frac{7}{2}$ and $S=\infty$ differ by no more than about 1% in the regime of R of interest here, Fig. 9. Moreover it is gratifying to note that for $x=1$ the two additional terms of the available series do not change our estimates for T_c obtained with terms up to $(1/k_BT)^4$ only. Since the Monte Carlo work allows to estimate $T_c(x)$ with an accuracy of 1% only, it makes sense to compare it to results for $S=\frac{7}{2}$ obtained experimentally for EuS [13]. Figure 10 shows typical Monte Carlo results for the temperature dependence of the magnetization, obtained for lattices with $N=10^3$ or 16^3 sites and periodic boundary conditions. For $x \gtrsim 0.7$ there is little dependence on N in the data below $T_c(x)$, while for $x \leqq 0.6$ there is a more pronounced size dependence. For $x \geqq 0.6$ we can obtain fairly accurate estimates for $T_c(x)$ from the inflection point of these curves, while this procedure becomes quite ambiguous for smaller x. While these data are obtained from simulations with periodic boundary conditions, for $x=1$ we have made runs with the "selfconsistent effective field" boundary condition [34] as well. The results for T_c obtained via both methods are identical, Fig. 11, and within their error (size of the points in Fig. 11) these results do agree with the series estimates shown in Fig. 9. Hence we feel that the errors involved in our various numerical procedures are fairly well-understood and small enough to allow us drawing meaningful conclusions. The accuracy of other approaches like generalizations of the constant-coupling approximation [35] or Green's function decoupling methods, which were applied to pure [36] and dilute [37] Heisenberg magnets, seems to us somewhat uncertain. But it is interesting to note that the predictions for $T_c(R)$ and $T_c(x)$ obtained from these approaches are qualitatively consistent with our work.

Figure 12 shows our estimates for $T_c(x)$ plotted vs. x in the case of $R=-\frac{1}{2}$. These estimates agree with the series estimates where the latter are meaningful ($x \gtrsim 0.7$). A discussion of the experimental data included in Fig. 12 is deferred to the next section. We here only note that the specific heat singularity at T_c which in simulation (and experiment) is quite pronounced in the pure case (Fig. 13) becomes strongly washed out in the diluted system. For $x \lesssim 0.8$ not even a remnant of the sharp anomaly at $T_c(x)$ is seen, but

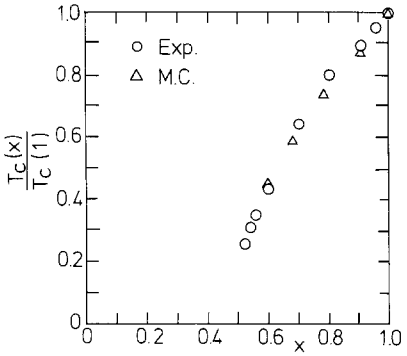

Fig. 12. Monte Carlo estimates for $T_c(x)$ plotted versus x for $R=-\frac{1}{2}$. Experimental data for $Eu_xSr_{1-x}S$ [13] are included

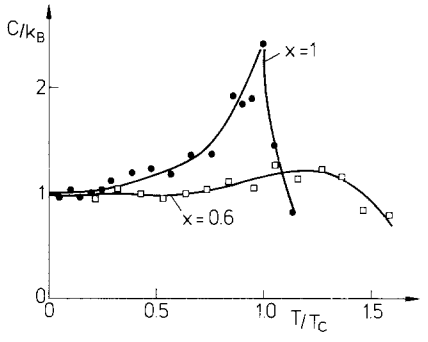

Fig. 13. Monte Carlo estimates for the specific heat as a function of normalized temperature in the pure and the dilute fcc Heisenberg model for $R=-\frac{1}{2}$

rather a broad Schottky-like anomaly at a temperature somewhat higher than $T_c(x)$ occurs. *A* similar effect was noted in real space renormalization group calculations for dilute (non-competing) Ising ferromagnets [38]. In our case this effect is even more pronounced because there are antiparallel and loose clusters in the percolating network which contribute to the specific heat but not to the magnetization (see Sect. II).

IV. Application to $Eu_xSr_{1-x}S$

EuS is considered to be a model substance for Heisenberg ferromagnetism and is believed to have nearest neighbor ferromagnetic and next nearest neighbor antiferromagnetic exchange, where $T_c=16.5\,\mathrm{K}$, $T_c/\Theta=0.81$ [33] (i.e. $\Theta=20.3\,\mathrm{K}$). From various measurements it was concluded that $R\approx-\frac{1}{2}$ [33]. These statements seem to be in conflict with our results, because using $\Theta=20.3\,\mathrm{K}$ and $R=-\frac{1}{2}$ we would predict $T_c\approx13.6\pm0.4\,\mathrm{K}$, which strongly disagrees with the experimental result. Within the frame of this model, we can reconcile these values for T_c and Θ with each other only if $R\approx0$ (Fig. 9), which is unreasonable in view of the experimental evidence for $R\approx-\frac{1}{2}$ in the pure EuS [33], and the occurrence of a spin glass phase in diluted EuS [13]. The conclusion is: either the numbers quoted are wrong, or the model is too simple.

In fact, there have been some suggestions that this simple model is not correct and the range of the antiferromagnetic superexchange is somewhat larger, extending to 3rd and 4th nearest neighbors as well [39]. In view of the fact that there are only 6 next-nearest neighbors a distance 1.0 a apart, but 24 3rd-nearest neighbors at a distance 1.22 a, 12 4th-nearest neighbors at a distance 1.41 a, etc., this suggestion seems quite reasonable. To investigate the consequences of this effect, we have included the 3rd-nearest neighbor exchange J_3 into our high-temperature analysis including terms up to $(1/k_BT)^3$, and keeping the paramagnetic Curie temperature Θ

$$\Theta=\frac{S(S+1)}{3k_B}(12J_1+6J_2+24J_3) \tag{2}$$

fixed as well as the ratio $\tilde{R}=(6J_2+24J_3)/12J_1=-\frac{1}{4}$ (which yields $R=-\frac{1}{2}$ if $J_3=0$). I.e., we redistribute the total negative interaction now over both second and third nearest neighbors, which would also be consistent with most of the evidence for the negative exchange interactions [33]. From Fig. 14 we see, however, that this does not change our estimate for $T_c\approx13.6\,\mathrm{K}$ at all. In fact, most of the physical consequences of having (weaker) negative exchange to both 2nd and 3rd neighbors are more or less the same as having (stronger) negative exchange to 2nd neighbors only, although some of the details shown in Fig. 1, 2 change.

An interaction of still larger range is provided by the magnetic dipolar interaction. Swendsen [36] has already suggested that this interaction must be included in an analysis of T_c/Θ for the Eu monochalcogenides, and suggests $R=-0.1$ for EuS. We think his analysis is misleading in several respects (i) claiming that the dipolar interaction can be treated in mean field approximation, which yields $T_c/\Theta\equiv1$, he just enhances the values for T_c/Θ without dipolar interaction by the fraction the dipolar energy makes to the total magnetic energy. However, while (uniaxial) dipolar ferromagnets have mean-field exponents (apart from logarithmic correction factors [40]), fluctuations do reduce T_c in comparison with Θ. For certain dipolar Ising ferromagnets Monte Carlo calculations yielded $T_c/\Theta\approx0.5$ [41]. For fcc dipolar Heisenberg ferromagnets no estimates for T_c/Θ are available, but we expect T_c/Θ again to be distinctly smaller than unity. Since dipolar interactions renor-

malize both Θ and T_c and a redistribution of interactions as discussed above had no effect on T_c/Θ, is is reasonable to neglect the effect of dipolar interactions on T_c/Θ for EuS. (ii) Swendsen's numerical estimate for R is based on a value of $\Theta = 19\,\mathrm{K}$ which is too low. As we shall see below, the use of experimental values of Θ determined in the traditional way by fitting susceptibility data at high temperatures to a Curie-Weiss law may be misleading.

Since there is no way to reasonably modify the model to make it fit to the mentioned results $T_c = 16.5\,\mathrm{K}$, $\Theta = 20.3\,\mathrm{K}$, it is natural to suspect that these numbers are inappropriate. While T_c is known to quite high precision there is in fact considerable uncertainty with respect to Θ: if recent high-precision data for the susceptibility of EuS measured from $T = 50\,\mathrm{K}$ to about $T = 250\,\mathrm{K}$ [16] are fitted to the traditional Curie-Weiss form

$$\chi = \frac{C}{T-\Theta} + \chi_{\mathrm{dia}}, \tag{3}$$

one obtains $\Theta = 19.5 \pm 0.2\,\mathrm{K}$, which would yield an even higher ratio T_c/Θ. At the same time the Curie constant C becomes enhanced by several percent over its theoretical value [16], and the diamagnetic susceptibility χ_{dia} is too large by several orders of magnitude. Hence although Eq. (3) represents the data reasonably accurate, this fit is a misleading procedure. A careful analysis of the data reveals the following facts [16]: (i) rather than by Eq. (3) the susceptibility in the high temperature region should be represented by the following formula

$$\chi(T,x) = \chi_{\mathrm{dia}} + \frac{xC}{T-\Theta x} \cdot \left\{1 - c_2(x)\left(\frac{\Theta x}{T}\right)^2 - c_2(x)\left(\frac{\Theta x}{T}\right)^3 - \ldots\right\} \tag{4}$$

where C has its theoretical value $\{C = N\mu_B^2 S(S+1)/3k_B\}$ and the coefficients $c_i(x)$ are related to the high temperature expansion coefficients (for details see Appendix B) (ii) due to thermal expansion (between $T = 100\,\mathrm{K}$ and $T = 250\,\mathrm{K}$ the lattice parameter is enhanced by about 0.5% [39]) and/or due to dilution (from $x = 1$ to $x = 0$ the lattice parameter changes by about 1% [16]) the exchange constants become slightly dependent on both dilution and temperature. This fact is seen from the observed pressure-dependence of T_c [42], and quantitatively explains the experimental deviations from the linear relation $\Theta(x) = \Theta x$ implied by Eq. (4) (for more details see [16]). Taking these facts into account, the data are now best fitted by the value $\Theta \approx 23\,\mathrm{K}$ [16], and from Fig. 9 we finally can conclude that $R = -0.45 \pm 0.05$, which justifies the use of $R = -0.5$ in most of our numerical calculations. This value is also supported by the good agreement between computer simulation and experiment, as far as the concentration dependence of T_c is concerned (Fig. 12). Note that Fig. 12 does no more involve any adjustable parameter.

An analysis of similar spirit as done here was done by Menyuk et al. [43] for EuO, fitting data in the range from 150 K to 300 K to high temperature series expansions [32]. Qualitatively similar to the findings of [16] a larger value for Θ was obtained than would follow from the traditional analysis (via Eq. (3)) from the same data. However, these authors disregarded thermal expansion effects which should have a pronounced effect for EuO in the studied temperature interval as well.

We then comment on the renormalization group analysis of Aharony [44] on the phase diagram of diluted Heisenberg magnets with additional dipolar interactions. He finds that the fixed point of such systems is unstable for $d < 4$, just as for random fields in Heisenberg systems [45], which implies that these systems rather behave as spin glasses. On the other hand, Aharony finds that cubic anisotropy stabilizes the otherwise unstable fixed point again, and hence he suggests that $T_c(x)$ should be determined by a delicate balance of randomness, dipolar interaction and cubic anisotropy. We feel, however, that this analysis does not apply to $Eu_xSr_{1-x}S$: there the dipolar interaction is quite small, and the cubic anisotropy is extremely small. Without these perturbations a sharp transition at the $T_c(x)$ as found from Monte Carlo and series expansions would result. The fact that the fixpoint associated with this transition becomes unstable when the dipolar force is added now means, in our interpretation, that the transition becomes *weakly* rounded. The stabilizing effect of the cubic anisotropy could then mean that somewhere on these rounded anomalies, whose positions are given by J_1, J_2 and x alone, there is superimposed a sharp anomaly (with amplitude related to the strength of the cubic anisotropy). This latter effect is quite irrelevant experimentally where one does find somewhat smeared transitions.

Finally we mention that our analysis implies for the structure of the ferromagnetic phase (Figs. 2, 3) that for $T \to 0$ the spontaneous magnetization should be smaller than the saturation magnetization $(= g\mu_B NSx)$, because of the antiparallel and loose spins and clusters. This effect has been also seen experimentally [15], and the magnitude of this reduction is in fair agreement with the prediction of the simulation for $R = -\frac{1}{2}$ (Fig. 6 A).

V. Conclusions

We summarize the main findings of this investigation as follows:

(i) In Ising or Heisenberg ferromagnets with competing exchange (such as nearest neighbor exchange ferromagnetic, next nearest neighbor exchange antiferromagnetic) dilution leads to a breakdown of ferromagnetic order before the percolation threshold is reached, and a spin glass phase appears. The precise location of the phase boundaries paramagnet-spin glass, paramagnet-ferromagnet and spin glass-ferromagnet depends on the interaction ratio R in a sensitive way. In particular, when R reaches its multicritical value (where ferromagnetism and antiferromagnetism coexist in the ground state of the pure system), we predict that arbitrarily small dilution already destroys these phases and rather stabilizes a spin glass, consisting of very large ferromagnetic and antiferromagnetic clusters coupled irregularly together. While concentration expansions can locate these phase boundaries only very crudely, even if one considers the ground state of the Ising square lattice which conceivably is the simplest case, Monte Carlo simulations can yield these phase boundaries with reasonable accuracy.

(ii) Due to the competing interactions not all spins in the percolating network are aligned parallel in the "ferromagnetic" regime, but some of them are aligned antiparallel. Sometimes due to the "frustration" of bonds no unique alignment is possible, but rather magnetic clusters occur within the surrounding ferromagnetic network, which have several degenerate ground states. Thus the ferromagnetic phase has an anomalously enhanced ground state entropy. In fact, it is plausible that at the critical value x_c'' where ferromagnetism and spin glass coexist the entropy $S_{FM}^{(0)}$ of the ferromagnetic phase exceeds the entropy $S_{SG}^{(0)}$ of the spin glass there: some of the clusters which would be loose if their environment has to be ferromagnetic can become aligned to the network again, if some other irregular spin structure in their environment is permitted. Thus, although on large length scales the degeneracy of the spin glass ground state is enhanced as compared to the ferromagnet, at smaller scales it should be strongly reduced. From this argument we immediately predict the observed negative slope of the spin glass-ferromagnet phase boundary dx_c''/dT at $T=0$ [7, 8]. Since $x_c''(T)$ is given by equating the free energies of the two phases, $F_{FM}(x,T) = F_{SG}(x,T)$, we have to linear order (U_{FM}, U_{SG} are the corresponding internal energies)

$$U_{FM}(x,0) - TS_{FM}(x,0) = U_{SG}(x,0) - TS_{SG}(x,0), \quad x = x_c''(T). \tag{5}$$

Note that we could omit the terms $T\left.\frac{\partial U}{\partial T}\right|_{T=0} = TC(T=0)$ because $C \propto T^{3/2}$ in the ferromagnet (for $S<\infty$) and $C \propto T$ in the spin glass phase [46]. Since we have

$$U_{FM}(x,0) - U_{SG}(x,0) = A[x_c''(T=0) - x], \tag{6}$$

where A is a constant, we find from (5) that $[x_c'' \equiv x_c''(T=0)]$

$$x_c'' - x_c''(T) = T[S_{FM}(x_c'',0) - S_{SG}(x_c'',0)]/A, \tag{7}$$

where we neglected terms of second order $\{[x_c'' - x_c''(T)]T\}$. Hence we predict {note $A>0$}

$$dx_c''/dT|_{T=0} = -[S_{FM}(x_c'',0) - S_{SG}(x_c'',0)]/A, \tag{8}$$

i.e. the negative slope is given by the entropy difference.

(iii) It is shown that the transition from the ferromagnetic to the paramagnetic phase $\{T_c(x)\}$ in $Eu_xSr_{1-x}S$ can be accounted for quantitatively by our simple model with $R \cong -\frac{1}{2}$. Exchange with more distant neighbors, the dipolar interaction as well as the cubic anisotropy are suggested to have insignificant effects on $T_c(x)$ only. A high temperature series analysis is used to remove apparent discrepancies between the experimental ratio between ferro- and paramagnetic Curie temperatures T_c/Θ and the theoretical one (see also Ref. 16). However, we do expect that the dipolar interaction should be relevant for the transition from the paramagnetic to the spin glass phase at nonzero temperatures, since the existence of spin glass phases for isotropic Heisenberg magnets is doubtful [12, 47]. From the quantitative analysis of the x-dependence of the susceptibility we obtain further evidence for the random character of the dilution in $Eu_xSr_{1-x}S$.

This work has benefitted from numerous stimulating discussions with U. Köbler, H. Maletta and W. Zinn.

Note Added in Proof: Similar Monte Carlo results for a diluted bcc lattice with $J_1>0$, $J_2<0$ were recently obtained by G.S. Grest, preprint.

Appendix A. Concentration Expansions

Here we consider a square Ising lattice with nearest neighbor exchange $J_1>0$, next nearest neighbor exchange $J_2<0$, with a concentration x of magnetic sites at $T=0$. First we consider the expansion of the susceptibilities defined in (1) in powers of x. For $x<x_p^{nn}=0.41$ [19] all spins belong to finite clusters. A cluster is defined as a group of exchange-coupled atoms. Each cluster configuration k can be characterized by its size s_k, its perimeter t_k, its magnetization m_k and its spin glass order parameter ψ_k. (For discussing χ_{SAF} [Eq. (1d)] it is convenient to also in-

troduce order parameters of the superantiferromagnetic phase, but for simplicity χ_{SAF} will not be considered further). Hence s_k is the number of spins in the cluster and t_k the number of non-magnetic lattice sites which are nearest or next-nearest neighbors to spins of the cluster. If each lattice site is occupied randomly with probability x, as we assume from now on, then the cluster concentration

$$c_k = x^{s_k-1}(1-x)^{t_k} \tag{A1}$$

is the average number per spin of such clusters. (Of course, there exist in general many different cluster configurations k with the same size s_k and the same perimeter t_k, for example mirror images of the cluster configuration).

The magnetization of the cluster k is $m_k = \sum_{i=1}^{s_k} S_i$ in the ground state. Trivially, every ground state is at least two-fold degenerate, since its interaction energy remains unchanged if all spins S_i reverse their orientation. But, due to frustration effects there may be many degenerate ground states, and we will need an average $\langle m_k^2 \rangle$ over all L different ground states of the cluster. Thus in searching for ground states we keep the first spin rigidly up and look through all remaining 2^{s_k-1} configurations of the spins in the cluster. Those with the lowest energy are ground states, which we denote by $\{S_i^l\}$, $l=1,\ldots,L$ (for clusters which do not contain loops we have $L=1$).

The order parameter ψ_k is defined as $\psi_k = \sum_{i=1}^{s_k} S_i S_i^l$ [2], and again an average $\langle \psi_k^2 \rangle$ over all L different ground states of the cluster will be needed. We can express the susceptibilities introduced in (1a–c) as [22]

$$k_B T \chi_F = x \sum_k c_k \langle m_k^2 \rangle, \tag{A2}$$

$$k_B T \chi_{EA} = k_B T \chi_{SG} = x \sum_k c_k \langle \psi_k^2 \rangle, \tag{A3}$$

while a "susceptibility" measuring the percolation of clusters would be

$$k_B T \chi_p = x \sum_k c_k s_k^2. \tag{A4}$$

One easily proves (A2), (A3) by inserting the definitions of m_k and ψ_k and noting from (1) that there is no correlation between any spins belonging to different clusters.

While χ_p has been considered for a long time in our case [19], χ_F and χ_{SG} have to our knowledge not yet been considered in previous work. While for $J_2 > 0$ we have $L=1$ and, then trivially $\langle m_k^2 \rangle = \langle \psi_k^2 \rangle = s_k^2$, the situation for $J_2 < 0$ is much more cumbersome, since all the clusters with same s_k but different structure have to be considered separately.

The susceptibilities are then expanded as power series in the concentration x as

$$k_B T \chi_F = x \sum_k \langle m_k^2 \rangle x^{s_k-1}(1-x)^{t_k} = x \left(1 + \sum_{n=1}^{\infty} a_n^F x^n\right), \tag{A5}$$

$$k_B T \chi_{SG} = x \sum_k \langle \psi_k^2 \rangle x^{s_k-1}(1-x)^{t_k} = x \left(1 + \sum_{n=1}^{\infty} a_n^{SG} x^n\right), \tag{A6}$$

$$k_B T \chi_p = x \sum_k s_k^2 x^{s_k-1}(1-x)^{t_k} = x \left(1 + \sum_{n=1}^{\infty} a_n^p x^n\right). \tag{A7}$$

Thus to get all series expansion coefficients a_n^p, a_n^F and a_n^{SG} up to $n=8$ we have to evaluate all clusters with sizes s_k up to 9. (The a_n^p are known from previous work [48] and were recalculated as a check; Tables of cluster numbers as a function of size ($s_k \leqq 10$) and perimeter t_k are published elsewhere [49]). Our computer program to find all configurations k followed Martin [50] where in most cases by going from one configuration to the next one only one of the s_k spins is moved. For the evaluation of ground state properties the computer time was reduced to about one fourth by not searching through the 2^{s_k-1} ground states separately for each configuration, but by storing first the interaction energies and magnetizations of the $s_k - 1$ "fixed" spins (with 2^{s_k-2} configurations). Then only the two possible orientations of the moving last site are taken into account together with its interaction with the other, fixed, spins. Nevertheless, for each unit added to the maximum cluster size, the computer time increased by about one order of magnitude, and reached about one hour for clusters of size 9 on the CDC Cyber 76 computer, where more than one million configurations were analyzed. This procedure is repeated independently for many different ratio's R of exchange energies. The results were checked by hand up to $n=3$. Tables A1, A2 list the expansion coefficients for the three series. Direct inspection shows already that $R=-\frac{1}{2}$ seems to be a rather special case. Our expansion coefficients a_n^p agree with that of Ref. 46 (available up to $n=7$). It is seen that the series obtained are quite irregular, particular for larger n, and hence their analysis is difficult.

Just as the divergence of $\chi_p(x)$ indicates the geometric transition at the percolation threshold x_p^{nnn}, we hope that the onset of ferromagnetism is characterized by a divergence of $\chi_F(x)$, and the onset of spin glass ordering by a divergence of $\chi_{SG}(x)$. Ratio plots do not

Table A1. Series expansion coefficients[a] a_n^p and a_n^{SG} for various R

	n	1	2	3	4	5	6	7	8
	a_n^p	8	32	108	348	1,068	3,180	9,216	26,452
	n	1	2	3	4	5	6	7	8
	R								
a_n^{SG}	0.001	8	32	108	298.2	996.9	2,419.7	8,766.2	10,968.4
	0.200	8	32	108	298.2	996.9	2,419.7	8,766.2	10,968.4
	0.333	8	32	108	298.2	996.9	2,419.7	9,085.4	9,977.3
	0.334	8	32	108	298.2	1,252.9	1,831.2	12,081.0	2,735.3
	0.400	8	32	108	298.2	1,252.9	1,831.2	11,886.8	3,104.7
	0.499	8	32	108	298.2	1,252.9	1,831.2	12,450.8	1,796.7
	0.500	8	32	52	159.7	624.8	−799.2	5,808.9	−25,308.1
	0.501	8	32	108	180	1,508	255.2	15,291.4	−19,125.7
	0.600	8	32	108	180	1,508	63.2	15,257.6	−21,051.0
	0.666	8	32	108	180	1,508	255.2	15,099.4	−18,471.5
	0.667	8	32	108	180	1,266.2	1,357.5	11,114.5	− 6,288.8
	0.800	8	32	108	180	1,266.2	1,261.5	11,570.5	− 7,480.8
	0.999	8	32	108	180	1,266.2	1,261.5	11,570.5	− 7,480.8
	1.000	8	10.7	104.4	64.8	325.5	2,387.8	−4,137.2	18,280.2
	1.001	8	16	116	100	640	2,400	32	15,952
	1.500	8	16	116	100	640	2,400	32	15,952
	2.000	8	16	116	100	640	2,400	−728.3	24,207.6
	3.000	8	16	116	100	640	2,400	−648	23,484
	4.000	8	16	116	100	640	2,400	−648	23,484
	5.000	8	16	116	100	640	2,400	−648	23,484

[a] In case of nonintegral coefficients only one digit behind the decimal point is shown.

Table A2. Series expansion coefficients[a] a_n^F for various R

R	n 1	2	3	4	5	6	7	8
0.001	0	16	− 20	97.3	− 177.3	602.4	− 872.4	1,740.7
0.200	0	16	− 20	97.3	− 177.3	602.4	− 872.4	1,740.7
0.333	0	16	− 20	97.3	− 177.3	602.4	− 927.5	2,148.5
0.334	0	16	− 20	97.3	− 337.3	1,658.4	− 6,788.8	27,506.7
0.400	0	16	− 20	97.3	− 337.3	1,658.4	− 6,898.1	28,058.7
0.499	0	16	− 20	97.3	− 337.3	1,658.4	− 7,226.1	30,098.7
0.500	0	16	− 76	318.1	1,163.8	4,087.1	−14,074.3	47,625.4
0.501	0	16	−132	628	−2,372	8,514.4	−32,161.6	125,267.0
0.600	0	16	−132	628	−2,372	8,322.4	−31,388.3	123,827.0
0.666	0	16	−132	628	−2,372	8,130.4	−30,401.6	121,715.0
0.667	0	16	−132	436	− 969.3	2,754.4	−10,994.9	37,061.7
0.800	0	16	−132	436	−1,041.3	3,474.4	−14,786.9	52,541.7
0.999	0	16	−132	436	−1,041.3	3,474.4	−14,786.9	52,541.7
1.000	0	−5.3	6.7	4	76.4	−686.8	2,760.8	−8,188.9
1.001	0	−16	76	−172	32	1,328	− 5,568	11,444
1.500	0	−16	76	−172	32	1,328	− 5,568	11,444
2.000	0	−16	76	−172	32	1,328	− 5,638.4	12,336.8
3.000	0	−16	76	−172	32	1,328	− 5,656	12,532
4.000	0	−16	76	−172	32	1,328	− 5,656	12,532
5.000	0	−16	76	−172	32	1,328	− 5,656	12,532

[a] In case of nonintegral coefficients only one digit behind the decimal point is shown.

work for χ_F and χ_{SG}. Thus instead we used the [4, 3] and [3, 4] Padé approximants to the logarithm of the susceptibilities in order to estimate the position of the singularities, i.e. the critical concentrations x_c'' for ferromagetism and x_c' for spin glass ordering. Often the Padé approximant gave a pole at the negative real axis near $x=-0.2$. Thus we expanded in the transformed variable [51] $u(x)=x/(x+y)$ with y

about 0.2 in order to get better results. The expansion coefficients thus were transformed as

$$1+\sum_{n=1}^{\infty} a_n x^n = 1+\sum_{n=1}^{\infty} b_n u^n,$$

with

$$b_n = \sum_{n'=1}^{n} a_{n'} y^{n'} \binom{n-1}{n'-1}. \tag{A8}$$

The resulting estimates for x_c', x_c'' are shown in Fig. 5. Note that for $R < -\frac{1}{2}$ the behavior of x_c'' was very erratic and is not included. Using one term less in the series and smaller Padé's changed the results of Fig. 5 considerably particularly near $R = \frac{1}{2}$. Thus we did not attempt to determine any critical exponents.

An alternative method is to derive an expansion in terms of $q = 1 - x$ for the magnetization. We just have to consider the reduction of the magnetization which occurs near clusters of holes (Fig. 2). For the concentration of such clusters we have, from Eq. (A1) and invoking particle-hole symmetry,

$$c_k = q^{s_k - 1}(1-q)^{t_k}. \tag{A9}$$

Denoting by r_k the number of reversed spins occurring near a hole-cluster k, the reduction of the magnetization is

$$\Delta M = 2\sum_k c_k \langle r_k \rangle = 2\sum_{n=3}^{\infty} b_n^M q^n [b_1^M = b_2^M = 0] \tag{A10}$$

where again an average over degenerate ground state configuration has to be taken, in order to calculate $\langle r_k \rangle$ and the coefficients b_n^M. Inspection shows that also clusters k contribute where holes are more apart than nearest or next-nearest neighbor distances, i.e. "clusters" which do not contribute to (A2)–(A4) because they would correspond to disconnected configurations of atoms. Hence a computer calculation of the series in (A10) would be much more difficult, and has not been attempted. A calculation by hand (Table A3), which hence still may be subject to slight errors, already shows that the resulting series again are rather irregular. Inspection of the series shows that ΔM increases when $R \to -\frac{1}{2}$, as expected.

Table A3. Series expansion coefficients b_n^M for various intervals of R

Interval	n 3	4	5
$-\frac{1}{3} < R < 0$	0	1	−1
$-\frac{1}{4} < R < -\frac{1}{5}$	0	1	15
$-\frac{2}{7} < R < -\frac{1}{4}$	4	−31	177
$-\frac{1}{3} < R < -\frac{2}{7}$	4	−31	201
$-\frac{3}{8} < R < -\frac{1}{3}$	4	− 7	−7
$-\frac{2}{5} < R < -\frac{3}{8}$	4	− 7	5
$-\frac{1}{2} < R < -\frac{2}{5}$	4	− 7	73

Appendix B. High Temperature Series Expansions for Impure Heisenberg Magnets

We consider an (inhomogeneous) Heisenberg magnet with general range of interaction $\{J_{ij}\}$ between two spins at lattice sites i, j and spin quantum number S. We consider the correlation

$$g(\mathbf{R}_0, \mathbf{R}) = \langle S_0^z S_R^z \rangle. \tag{B1}$$

In a homogeneous system this correlation would be independent of $\mathbf{R}_0$. The bracket in (1) denotes a canonical thermal average,

$$\langle \ldots \rangle = \mathrm{Tr}\exp(-\mathscr{H}/k_B T)\ldots/\mathrm{Tr}\exp(-\mathscr{H}/k_B T), \tag{B2}$$

with

$$\mathscr{H} = -\tfrac{1}{2}\sum_{i \neq j} J_{ij}\mathbf{S}_i\mathbf{S}_j - g\mu_B H\sum_i S_i^z. \tag{B3}$$

In (3) the sums run over those lattice sites only which are occupied by magnetic atoms, if the system is diluted with nonmagnetic impurities.

The high temperature expansion of the correlation in (B1) is

$$g(\mathbf{R}_0, \mathbf{R}) = \sum_k 1/(k_B T)^k c_k(\mathbf{R}_0, \mathbf{R}). \tag{B4}$$

Formal expressions for the $c_k(\mathbf{R}_0, \mathbf{R})$, $k \leqq 5$ have already been derived in [52]. Correcting some errors, the results are given in terms of infinite-temperature averages, denotes by $\langle \ldots \rangle_0$

$$X \equiv \langle (S^z)^2 \rangle_0 = S(S+1)/3,$$

$$Y = \langle (S^z)^4 \rangle_0 = \sum_{m=-s}^{+s} m^4/(2S+1) = X(9X-1)/5$$

as

$$c_0 = X J_{Or}, \quad c_1 = X^2 J_{OR},$$

$$c_2 = X^3 \sum_K J_{OK} J_{KR} - X^2 J_{OR}^2/4,$$

$$c_3 = X^4 \sum J_{OK} J_{KL} J_{LR} - X^3(\tfrac{1}{2}\sum J_{OK}^2 J_{KR} + \tfrac{1}{2}\sum J_{OK} J_{KR}^2 + J_{OR}\sum J_{KO} J_{KR} + J_{OR}\sum J_{OK}^2 + J_{OR}\sum J_{KR}^2)/6 + (6X^4 - 4X^3 - 12YX^2 + 4YX/3 + 10Y^2/3 + 2X^2/3) J_{OR}^3/8,$$

$$c_4 = X^5 \sum J_{OK} J_{KL} J_{LM} J_{MR} - X^4(2J_{OR}\sum J_{OK} J_{KL} J_{LO} + 2J_{OR}\sum J_{RK} J_{KL} J_{LR} + 2\sum J_{OL} J_{LR} J_{LK}^2 + \sum J_{OK}^2 J_{KL} J_{LR} + \sum J_{OK} J_{KL}^2 J_{LR} + \sum J_{OK} J_{KL} J_{LR}^2 + 2\sum J_{OK}^2 J_{OL} J_{LR} + 2\sum J_{OL} J_{LR} J_{KR}^2 + 2J_{OR}\sum J_{OK} J_{KL} J_{LR})/12 + X^3(J_{OR}\sum J_{OK}^3 + J_{OR}\sum J_{KR}^3)/24 + X(18X^4 - 12X^3 + 2X^2 - 36YX^2 + 4YX + 10Y^2)(J_{OR}^2 \sum J_{OK} J_{KR}$$

$$+\tfrac{1}{3}\sum J_{OK}^3 J_{KR}+\tfrac{1}{3}\sum J_{OK}J_{KR}^3)/8$$
$$+X^2(6X^2+\tfrac{1}{3}X-\tfrac{10}{3}Y)(J_{OR}^2\sum J_{OK}^2+J_{OR}^2\sum J_{KR}^2)/16$$
$$+(-\tfrac{47}{4}X^4+\tfrac{9}{2}X^3-\tfrac{5}{12}X^2+\tfrac{43}{2}YX^2-\tfrac{11}{6}YX$$
$$-\tfrac{85}{12}Y)J_{OR}^4/16 \qquad \text{(B5)}$$

and the expression for c_5 is too involved to be reported here. In (B5), it is understood that lattice sites O, R, K, L, M are all magnetic sites (i.e., no impurity sites), and in each sum different from each other. We now specialize to the case of an ideal randomly quenched mixture of magnetic ions (at concentration x) with nonmagnetic ones, and consider the correlation function

$$g_{\mathrm{av}}(\mathbf{R})=[g(\mathbf{R}_0,\mathbf{R})]_{\mathrm{av}} \qquad \text{(B6)}$$

averaged over the disorder. From (B4, B5) we then derive the series expansion

$$g_{\mathrm{av}}(\mathbf{R})=\sum_k 1/(k_BT)^k c_k^{\mathrm{av}}(\mathbf{R},x),$$
$$c_k^{\mathrm{av}}(\mathbf{R},x)=\sum_{l=0}^{k} c_{lk}(\mathbf{R})\,x^{2+1}, \qquad \text{(B7)}$$

with [note that $c_{OK}(\mathbf{R})\equiv 0$ for $k\neq 0$]

$$c_{00}(\mathbf{R})=X\delta_{OR}, \quad c_{11}(\mathbf{R})=X^2J_{OR},$$
$$c_{12}(\mathbf{R})=-X^2J_{OR}^2/4, \quad c_{22}(\mathbf{R})=X^3\sum J_{OK}J_{KR},$$
$$c_{13}(\mathbf{R})=-(3X^4+X^3-X^2/3)J_{OR}^3/5,$$
$$c_{23}(\mathbf{R})=-X^3(\tfrac{1}{2}\sum J_{OK}^2J_{KR}+\tfrac{1}{2}\sum J_{OK}J_{KR}^2$$
$$+J_{OR}\sum J_{KO}J_{KR}+J_{OR}\sum J_{OK}^2+J_{OR}\sum J_{KR}^2)/6,$$
$$c_{33}(\mathbf{R})=X^4\sum J_{OK}J_{KL}J_{LR},$$
$$c_{14}(\mathbf{R})=(4X^4+2X^3-X^2/3)J_{OR}^4/16,$$
$$c_{24}(\mathbf{R})=X^3(J_{OR}\sum J_{OK}^3+J_{OR}\sum J_{KR}^3)/24$$
$$-3X(3X^4+X^3-X^2/5)(J_{OR}^2\sum J_{OK}J_{KR}+\tfrac{1}{3}\sum J_{OK}^3J_{KR}$$
$$+\tfrac{1}{3}\sum J_{OK}J_{KR}^3)/5+X^3(J_{OR}^2\sum J_{OK}^2+J_{OR}^2\sum J_{KR}^2)/16,$$
$$c_{34}(\mathbf{R})=-X^4(2J_{OR}\sum J_{OK}J_{KL}J_{LO}+2J_{OR}\sum J_{RK}J_{KL}J_{LR}$$
$$+\sum J_{OK}^2J_{KL}J_{LR}+2\sum J_{LK}^2J_{OL}J_{LR}+\sum J_{OK}J_{KL}^2J_{LR}$$
$$+\sum J_{OK}J_{KL}J_{LR}^2+2\sum J_{OK}^2J_{OL}J_{LR}+2\sum J_{OL}J_{LR}J_{KR}^2$$
$$+2J_{OR}\sum J_{OK}J_{KL}J_{LR})/12,$$
$$c_{44}(\mathbf{R})=X^5\sum J_{OK}J_{KL}J_{LM}J_{MR}. \qquad \text{(B8)}$$

Note that in the sums in (B8) *all* lattice sites may occur, there is no longer any restriction to magnetic sites due to the averaging process.

The series expansion for the averaged magnetic susceptibility χ_{av}^{zz} per site becomes

$$k_BT\chi_{\mathrm{av}}^{zz}=(g\mu_B)^2\sum_R g_{\mathrm{av}}(\mathbf{R})$$
$$=(g\mu_B)^2X\sum_k 1/(k_BT)^k a_k^{\mathrm{av}}(x), \qquad \text{(B9)}$$

with

$$a_k^{\mathrm{av}}(x)=\sum_{l=0}^{k} a_{lk}x^{l+1}, \quad a_{lk}=\sum_R c_{lk}(\mathbf{R})/X. \qquad \text{(B10)}$$

Expressions for internal energy, specific heat, static structure factor can be derived similarly but will not be considered here. The sums over interaction constants in (B8) can be conveniently calculated on the computer, for a given lattice structure and assumptions on the range of the interaction. We have calculated all $c_{lk}(\mathbf{R})$ for the *fcc* lattice with interactions between first, second and third nearest neighbors J_1, J_2, J_3 for $k\leqq 3$ and with interactions between first and second neighbors only for $k=4$. From these coefficients (which are too lengthy to be tabulated here) we calculated both the susceptibility series, Eqs. (B9, B10), and the series for the square of the correlation length (which can be expressed by the second moment of the correlations, as is well known [52]). We only quote here the susceptibility series explicitly, which is given by the following coefficients:

$$a_{00}=1, \quad a_{11}=X(12J_1+6J_2+24J_3),$$
$$a_{12}=-X(12J_1^2+6J_2^2+24J_3^2)/4,$$
$$a_{22}=X^2(132J_1^2+144J_1J_2+30J_2^2+576J_1J_3$$
$$+288J_2J_3+552J_3^2),$$
$$a_{13}=-(3X^3+X^2-X/3)(12J_1^3+6J_2^3+24J_3^3)/5,$$
$$a_{23}=-X^2(444J_1^3+288J_1^2J_2+216J_1J_2^2+90J_2^3$$
$$+1{,}008J_1^2J_3+1{,}008J_1J_3^2+144J_1J_2J_3+432J_2^2J_3$$
$$+576J_2J_3^2+1{,}704J_3^2)/6,$$
$$a_{33}=X^3(1{,}404J_1^3+2{,}376J_1^2J_2+1{,}152J_1J_2^2+150J_2^3$$
$$+9{,}648J_1^2J_3+20{,}160J_1J_3^2+10{,}244J_1J_2J_3$$
$$+2{,}520J_2^2J_3+9{,}576J_2J_3^2+12{,}648J_3^3),$$
$$a_{14}=(4X^3+2X^2-X/3)(12J_1^4+6J_2^4)$$
$$(J_3=0 \text{ here and in the following}),$$
$$a_{24}=X^2(264J_1^4+144J_1^3J_2+144J_1J_2^3+60J_2^4)/24$$
$$+X^2(264J_1^4+288J_1^2J_2^2+60J_2^4)/16-3(3X^4+X^3$$
$$-X^2/3)(136J_1^4+96J_1^3+24J_1^2J_2^2+48J_1J_2^3+20J_2^4),$$
$$a_{34}=-X^3(14{,}916J_1^4+19{,}728J_1^3J_2+12{,}456J_1^2J_2^2$$
$$+6{,}912J_1J_2^3+1{,}338J_2^4)/12,$$
$$a_{44}=X^4(14{,}700J_1^4+33{,}696J_1^3J_2+26{,}280J_1^2J_2^2$$
$$+7{,}920J_1J_2^3+726J_2^4). \qquad \text{(B11)}$$

Eq. (B11) agrees with several special cases obtained earlier: for $J_2=J_3=0$ it checks with the fcc lattice results of Morgan and Rushbrooke [29], for $J_1=J_3=0$ it yields their sc lattice results, while for $x=1$, $J_3=0$ one obtains the results of Pirnie et al. [32].

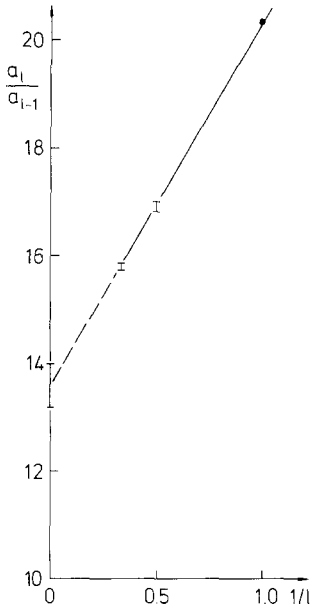

Fig. 14. Ratio plot for the susceptibility of an fcc $S=\frac{7}{2}$ Heisenberg ferromagnet with $\tilde{R}=-\frac{1}{4}$, $\Theta=20.3$ K. All ratios for $-\frac{1}{2}\leqq R\leqq 0$ fall within the "error bars" shown

From (B11), (B10) it is easy to obtain the coefficients $a_k(x)$ whose ratios were analyzed in Figs. 7, 14. Here we also consider a modified high temperatures series expansion, which is convenient for the comparison with experimental data, namely {cf. Eq. (4)}

$$\chi=\frac{N x(g\mu_B)^2 S(S+1)}{3k_B[T-\Theta(x)]}\left\{1-c_2(x)\left[\frac{\Theta(x)}{T}\right]^2 -c_3(x)\left[\frac{\Theta(x)}{T}\right]^3-c_4(x)\left[\frac{\Theta(x)}{T}\right]^3-\ldots\right\} \quad \text{(B12)}$$

From (B10)-(B12) we immediately find $k_B\Theta(x)=xa_{11}=xX(12J_1+6J_2+24J_3)$, by requiring that there is no linear term $(\Theta(x)/T)$ within the curly bracket of (B12). The coefficients $c_k(x)$ are related to the $a_k(x)$ by

$$c_k(x)=\frac{a_{k-1}(x)\,a_1(x)-a_k(x)}{a_1^k(x)}. \quad \text{(B13)}$$

E.g. for $J_3=0$ one obtains

$$c_2(x)=\frac{(1+R^2/2)\left(1+\dfrac{1}{4xX}\right)}{12(1+R+R^2/4)}$$

and

$$c_3(x)=\frac{3+2R+4R^2/3+11R^3/18+(8+16R/3+4R^2+5R^3/3)/(12xX)+\dfrac{(1+R^3)}{30x^2}[1+1/(3X)-1/(3X)^2]}{16+24R+12R^2+18R^3}-c_2(x)$$

etc. These expressions can be used to analyse the $Eu_xSr_{1-x}S$-data putting $X=S(S+1)/3=\frac{21}{4}$, and $R=J_2/J_1=-\frac{1}{2}$.

Finally we discuss the extension of our method to the case of non-random mixing. While (B5) still holds, the averaging process in (B6) has to take correlations in the geometric arrangement of magnetic atoms into account, and the $c_k^{\mathrm{av}}(\mathbf{R},x)$ in (B7) are no longer simple polynomials in x. Let us denote by $p_x(\mathbf{R})$ the conditional correlation that the site $\mathbf{R}$ is occupied by a magnetic atom if the origin is occupied by a magnetic atom. Then we find the first two expansion coefficients of $g_{\mathrm{av}}(\mathbf{R})$ as

$$c_0^{\mathrm{av}}(\mathbf{R},x)=xX\delta_{OR},\qquad c_1^{\mathrm{av}}(\mathbf{R},x)=xX^2\,p_x(\mathbf{R})J_{OR}. \quad \text{(B14)}$$

(In the case of random mixing $p_x(\mathbf{R})=x$ and we recover (B8). The higher order coefficients would involve also triplet, quadruplet - etc. rather than only pair probabilities.) From (B14), (B9) we find that

$$\chi=\frac{N x(g\mu_B)^2 S(S+1)}{3k_BT}\left\{1+\frac{\Theta(x)}{T}+\ldots\right\}, \quad \text{(B15)}$$

where (z_i is the coordination number of the i'th neighbor shell)

$$k_B\Theta(x)=X\sum_i z_iJ_i\,p_x(\mathbf{R}_i). \quad \text{(B16)}$$

Hence correlations in the arrangement of magnetic atoms show up as deviations of $\Theta(x)$ from linear variation with x. On the other hand, if $\Theta(x)=\Theta(1)x$, it follows that $p_x(\mathbf{R}_i)=x$ and the mixing must be random.

References

1. Recent theoretical reviews include: de Dominicis, C. In: Proc. Int. Conf. on Critical Dynamics. Enz, C.P. (ed.), to be published; Lubensky, T.C. In: Les Houches 1978 Lecture Notes, to be published; Kirkpatrick, S.: ibid; Stauffer, D.: Phys. Repts. **54**, 1 (1979); Blandin, A.: J. de Phys. **39C6**, 1499 (1978); Binder, K.: Festkörperprobleme (Advances in Solid State Physics) XVII, 55 (1977); and Ref. 2
2. Binder, K. In: Ordering in Strongly Fluctuating Condensed-Matter Systems. Riste, T. (ed.). New York: Plenum Press 1979
3. Recent experimental reviews include: Cowley, R.A., Guggenheim, G.A., Shirane, S.: in Ref. 2; Beck, P.A.: Progr. Mat. Sci. **23**, 1 (1978); Murani, A.P.: J. de Phys. **39**, C6-1517 (1978); Mydosh, J.A. In: Amorphous Magnetism II. Levy, R.A., Hasegawa, S. (eds.). New York: Plenum Press 1977

4. Computer simulations are reviewed by Binder, K.: J. de Phys. **39**, C6-1527 (1978), and by Binder, K. and Stauffer, D. In: Monte Carlo Methods in Statistical Physics. Binder, K. (ed.). Berlin-Heidelberg-New York: Springer 1979
5. See Stauffer, D.: Ref. 1; Kirkpatrick, S.: Ref. 1
6. See Lubensky, T.C.: Ref. 1; Cowley, R.A., et al.: Ref. 2
7. Coles, B.R., Sarkissian, B.V.B., Taylor, R.H.: Phil. Mag. B**37**, 489 (1978)
   Verbeek, B.H., Mydosh, J.A.: J. Phys. F**8**, L109 (1978)
8. Maletta, H., Convert, P.: Phys. Rev. Lett. **42**, 108 (1979)
9. de Dominicis, C.: Ref. 1; Blandin, A.: Ref. 1
10. See e.g. Beck, P.A.: Ref. 3, and Tholence, J.L., Holtzberg, F., Tournier, R. In: Amorphous Magnetism II. Levy, R.A., Hasegawa, S. (eds.). New York: Plenum Press 1977
11. Edwards, S.F., Anderson, P.W.: J. Phys. F**5**, 965 (1975)
12. Binder, K.: Z. Physik B**24**, 339 (1977)
13. Maletta, H., Felsch, W.: Phys. Rev. B**20**, in press
14. Eiselt, G., Kötzler, J., Maletta, H., Stauffer, D., Binder, K.: Phys. Rev. B**19**, 2664 (1979) and J. Mag. Magn. Mater., to be published
15. Köbler, U.: to be published
16. Köbler, U., Binder, K. In: Proceedings of the International Conference on Magnetism, Munich, Sept. 3-7, 1979, to be published
17. Binder, K., Kinzel, W., Maletta, H., Stauffer, D.: in Ref. 16.
18. Binder, K., Landau, D.P.: to be published
19. Dalton, N.W., Domb, C., Sykes, M.F.: Proc. Phys. Soc. (London) **83**, 496 (1964)
20. Toulouse, G.: Comm. Phys. **2**, 115 (1977)
21. Villain, J.: Z. Physik B**33**, 31 (1979)
22. Aharony, A., Binder, K.: in Ref. 16, and to be published
23. This was pointed out to us by B.I. Halperin
24. Griffiths, R.B.: Phys. Rev. Lett. **23**, 17 (1968)
25. Rapaport, D.C.: J. Phys. C**5**, 2813 (1972)
    Morgan, D.J., Rushbrooke, G.S.: Mol. Phys. **6**, 477 (1963)
26. Idogaki, T., Uryû, N.: J. Phys. Soc. Japan **43**, 845 (1977); J. Phys. Soc. Japan **45**, 1498 (1978)
27. Domb, C., Green, M.S. (eds.): Phase Transitions and Critical Phenomena, Vol. 3. New York: Academic Press 1974
28. Rapaport, D.C.: J. Phys. C**5**, 1830 (1972), and references therein
29. Rushbrooke, G.S., Morgan, D.J.: Mol. Phys. **4**, 1 (1961)
    Morgan, D.J., Rushbrooke, G.S.: Mol. Phys. **4**, 291 (1961)
30. Elliott, R.S., Heap, B.R.: Proc. Roy. Soc. A**265**, 264 (1962)
    Rushbrooke, G.S., Muse, R.A., Stephenson, R.L., Pirnie, K.: J. Phys. C**5**, 337 (1972)
31. Le Guillou, J.C., Zinn-Justin, J.: Phys. Rev. Lett. **39**, 95 (1977)
32. Pirnie, K., Wood, P.J., Eve, J.: Mol. Phys. **11**, 551 (1966)
33. de Jongh, L.J., Miedema, A.R.: Adv. Physics **23**, 1 (1974)
34. Müller-Krumbhaar, H., Binder, K.: Z. Physik **254**, 262 (1972)
    Binder, K., Müller-Krumbhaar, H.: Phys. Rev. B**7**, 3297 (1973). Note that this boundary condition using a (homogeneous) surface field is less appropriate for a strongly inhomogeneous system
35. Callen, H.B., Callen, E.: Phys. Rev. A**136**, 1675 (1964)
36. Swendsen, R.H.: Phys. Rev. B**5**, 116 (1972)
37. Dvey-Aharon, H., Fibich, M.: Phys. Rev. B**18**, 3491 (1978)
38. Jayaprakash, C., Riedel, E.K., Wortis, M.: Phys. Rev. B**18**, 2244 (1978)
39. Zinn, W.: J. Magn. Mat. **3**, 23 (1976)
40. Larkin, A.I., Khmelnitskii, D.E.: Sov. Phys. JETP **29**, 1123 (1969)
41. Kretschmer, R., Binder, K.: Z. Physik B **34**, 375 (1979)
42. Schwob, P., Vogt, O.: Phys. Lett. **24** A, 242 (1967)
43. Menyuk, N., Dwight, K., Reed, T.B.: Phys. Rev. B**3**, 1689 (1971)
44. Aharony, A.: to be published
45. Imry, Y., Ma, S.K.: Phys. Rev. Lett. **35**, 1399 (1975)
46. Meschede, D., Steglich, F., Felsch, W., Maletta, H., Zinn, W.: to be published
47. Stauffer, D., Binder, K.: in Ref. 16
48. Domb, C., Dalton, N.W.: Proc. Phys. Soc. **89**, 859 (1966)
49. Peters, H.P., Stauffer, D., Halters, H.P., Lovenich, K.: Z. Physik **B** (1979)
50. Martin, J.L. In: Phase Transitions and Critical Phenomena, Vol. III, p. 97. Domb, C., Green, M.S. (eds.). London: Academic Press 1974
51. Pearce, C.J.: Adv. Phys. **27**, 89 (1978)
52. Binder, K.: Thesis (Technical University of Vienna, 1969, unpublished). See also Binder, K.: phys. stat. solidi **32**, 891 (1969)

K. Binder
W. Kinzel
Institut für Festkörperforschung
Kernforschungsanlage Jülich GmbH
Postfach 1913
D-5170 Jülich 1
Federal Republic of Germany

D. Stauffer
Institut für Theoretische Physik
Universität zu Köln
Zülpicher Straße 77
D-5000 Köln 41
Federal Republic of Germany